

LA-UR -84-620

CONF-84/0255 -3

LA-UR--84-620

DE84 007492

Los Alamos National Laboratory is operated by the University of California for the United States Department of Energy under contract W-7405-ENG-36

TITLE: CONFINEMENT TIME AND ENERGY BALANCE IN THE CTX SPHEROMAK

AUTHOR(S) Cris W. Barnes, I(var)s Henins, H(iroshi) W. Huida,
T(homas) R. Jarboe, CTI-5

SUBMITTED TO 6th Symposium on Compact Toroid Physics Technology

DISCLAIMER

This report was prepared as an account of work sponsored by an agency of the United States Government. Neither the United States Government nor any agency thereof, nor any of their employees, makes any warranty, express or implied, or assumes any legal liability or responsibility for the accuracy, completeness, or usefulness of any information, apparatus, product, or process disclosed, or represents that its use would not infringe privately owned rights. Reference herein to any specific commercial product, process, or service by trade name, trademark, manufacturer, or otherwise does not necessarily constitute or imply its endorsement, recommendation, or favoring by the United States Government or any agency thereof. The views and opinions of authors expressed herein do not necessarily state or reflect those of the United States Government or any agency thereof.

MASTER

By acceptance of this article, the publisher recognizes that the U.S. Government retains a non-exclusive, royalty-free license to publish or reproduce the published form of this contribution or to allow others to do so for U.S. Government purposes.

The Los Alamos National Laboratory requests that the publisher identify this article as work performed under the auspices of the U.S. Department of Energy

Los Alamos

Los Alamos National Laboratory
Los Alamos, New Mexico 87545

Confinement Time and Energy Balance in the CTX Spheromak

Cris W. Barnes, I. Henins, H. W. Hoida, and T. R. Jarboe
Los Alamos National Laboratory
Los Alamos, NM 87545

The multipoint Thomson scattering diagnostic on CTX allows measurement of electron plasma pressure. The pressure correlates well with the poloidal flux function. Analysis using equilibrium models allows the $\langle\beta\rangle_{vol}$ to be calculated from over 100 Thomson scattering profiles taken under standard conditions of spheromak operation where the plasma parameters vary widely within the discharge. The calculated T_E increases with central core temperature and with density. The global magnetic energy decay time τ_B^2 is consistent with Spitzer-Harm resistivity, but with an anomaly factor of 2-4 which may decrease at small ratios of B/n . The nT_E product reaches $4 \times 10^9 \text{ s cm}^{-3}$ during the hottest part of the discharge. A zero-dimensional energy balance code, which accurately includes all the major atomic physics processes and whose parameters have been constrained by comparison to experimental data, is used to identify the causes of energy loss that contribute to the observed confinement time. The most important power loss is that needed to replace the particles being lost and to maintain the constant density of the plateau.

The multipoint Thomson scattering diagnostic on CTX^{1,2} provides radial profiles of electron temperature and density. The absolute value of the density is obtained by normalizing the data to values obtained from line-integrated laser interferometry.³ The measured electron pressure at each radial position is compared to the estimated poloidal flux ψ at that radius (Fig. 1) using equilibrium models to calculate the flux function. The errors in the measurement of the pressure result in scatter of the data that obviates any necessity to use accurate equilibrium models for ψ , which for our analysis¹ of $\langle p \rangle$ is assumed to be $\psi(r) = \sin(\pi r^2/R^2)$. Most Thomson scattering profiles result in good correlation of p with ψ as in Fig. 1.

The $\langle\beta\rangle_{vol} = \langle p \rangle_{vol}/\langle B^2/2\mu_0 \rangle_{vol}$ can be calculated from the pressure measurement and from magnetic field equilibrium models normalized to field or current measurements.¹ In the analysis of $\langle\beta\rangle_{vol}$ the ion pressure (as yet unmeasured to any accuracy) is assumed to be equal to the electron pressure. Over 100

Thomson scattering profiles with good fits across the radius have been obtained at different times during spheromak operation under a standard set of conditions. These discharges were formed using "slow" mode⁴ at 30 mT filling pressure¹ in the 40 cm radius mesh flux conserver³ with 25 bridges. About 30% of the data is from discharges where the source continued to operate at low currents ("mixed" mode⁵) but where the macroscopic variables were less than 10% different. The B , n , and T_E vary widely in magnitude during the decay of the discharge allowing comparison of confinement with changes in these variables. Care must be taken in interpreting the analysis since the variations in different parameters may be correlated with each other due to time dependence within the standard conditions. Figure 2 shows the $\langle\beta\rangle_{vol}$ versus time under the standard conditions. The $\langle\beta\rangle_{vol}$ reaches about 8% and remains somewhat constant during most of the hot portion of the discharge (0.3-0.6 ms). Late in time the temperature does not drop as fast as the B^2 while the density actually

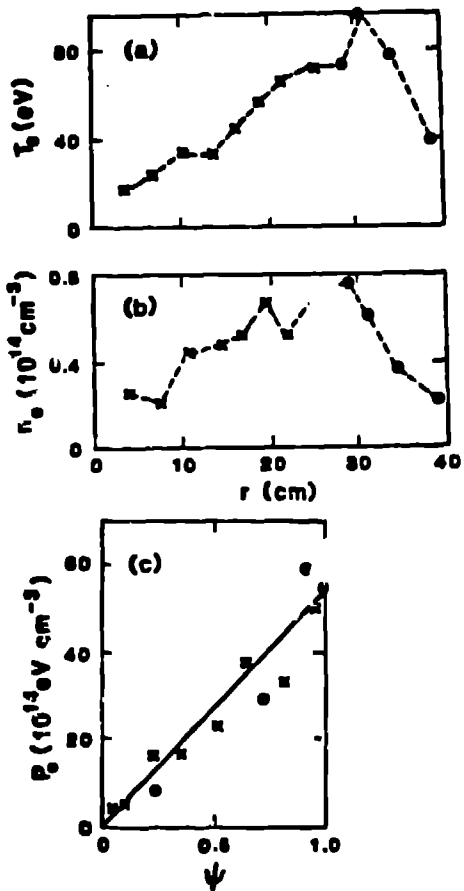


Fig. 1. (a-b) Multipoint Thomson scattering radial profiles of electron temperature and density. (c) Electron pressure versus poloidal flux calculated from an equilibrium model. The x's are from radial data inside the magnetic axis, and the o's are from outside.

increases and the $\langle\beta\rangle_{vol}$ goes up. This relative increase in confinement may be due to the ions becoming unmagnetized in the low fields late in time.

The decay of the magnetic field, which with τ_B^2 of only 300 μ s at central electron temperatures of over 100 eV seems anomalously short, may still be consistent with Spitzer-Härm resistivity.⁶ If the plasma decays self-similarly as it tries to maintain minimum-energy profiles^{4,7,8} the global magnetic energy decay time is expected to be $\tau_B^2 = \int B^2/2\mu_0 dV / \int n j^2 dV$. High

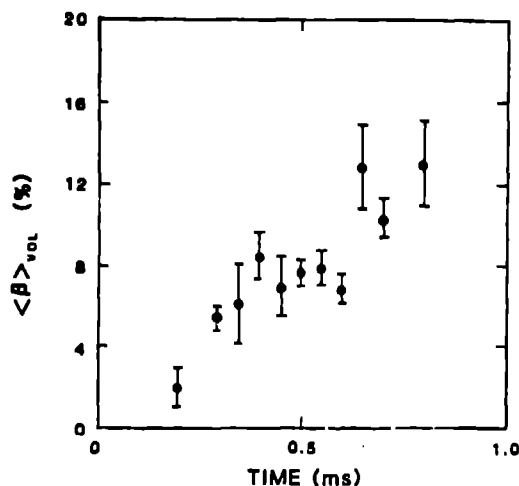


Fig. 2. $\langle\beta\rangle_{vol}$ versus time in the discharge. The value of $\langle\beta\rangle_{vol}$ from between 3 to 15 Thomson scattering profiles taken under standard conditions has been averaged at each time.

field and current density regions of large volume in the cold outer portions of a spheromak can weight these integrals and keep the expected "classical" τ_B^2 quite small. The classical τ_B^2 is calculated for different temperature profiles, and the results are shown in Figure 3. A zero-beta minimum-energy Bessel function model⁹ is used for the field, flux, and current distributions in space in a cylindrical pillbox with $R=L$. The resistivity is assumed to depend on the flux as $\eta = (c_1 + c_2\psi^\alpha)^{-1}$, with c_1 and c_2 chosen to make η match the classical value at a specified edge temperature (20 eV) and central temperature (varied up to 1 keV). (ψ is normalized to 1 at the magnetic axis.) For broad temperature profiles (α small) and not too cold edge temperatures, the classical $\tau_B^2 \propto \langle T_e \rangle^{3/2}$.

The correlation of τ_B^2 and $\langle T_e \rangle_{vol}$ can be compared experimentally. From the core temperature (representing an average over the innermost 25% of poloidal flux, from 21-35 cm) the $\langle T_e \rangle_{vol}$ can be crudely

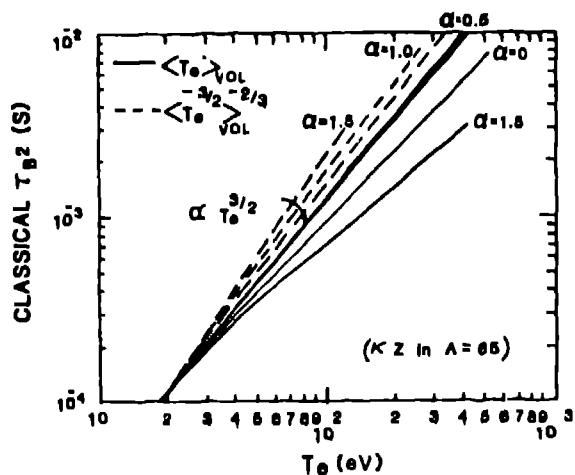


Fig. 3. The global magnetic energy decay time τ_B^2 expected from "classical" Spitzer-Harm resistivity, is plotted versus the volume-average temperature (solid lines) and the volume-(-2/3rd)-root-(-3/2)-mean temperature (dash). A value of $\kappa Z \ln \Lambda = 65$ has been assumed for the calculation, with $\ln \lambda (\sim 12)$ the Coulomb logarithm, $Z(\sim 1.5)$ is Z_{eff} times the S-H correction, and $\kappa(\sim 3.5)$ is the anomaly factor.

estimated by assuming $T_e = 20$ eV + const $\times \psi$, and using the fact¹ that $\langle \psi \rangle_{vol} = 0.41$. If $\kappa Z \ln \lambda = 65$ is assumed, the classical τ_B^2 is approximated as $\approx 1.22 \times (11 + 0.47 T_{core})^{1.4}$ using the results of Fig. 3. Figure 4 shows the result of comparing this to the actual experimentally measured $\tau_B^2 = \Delta t / \Delta \ln B^2$ over a $\pm 50 \mu s$ window about the time of the Thomson scattering pulse. There is a weak correlation, with wide scatter in the data consistent with the large error bars. It is interesting that the data appears bounded on the left by the no-anomaly, $\kappa=1$ -times-classical scaling. It is also suggestive that many shots with low ratios of peak- B/n_e (proportional to the current drift velocity) appear to have a low anomaly.

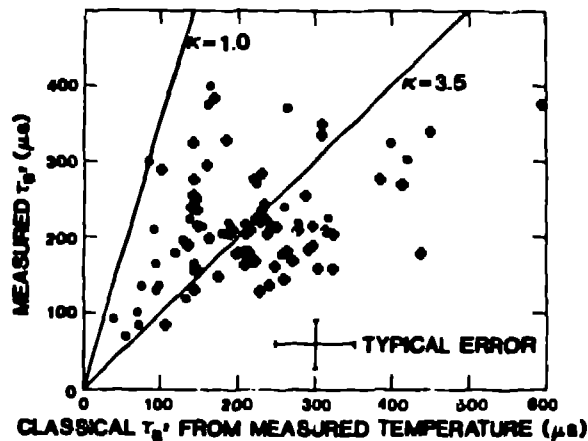


Fig. 4. Experimentally measured τ_B^2 from magnetic field decay, versus the "classical" τ_B^2 . The circles, which tend to lie at lower values of the anomaly κ , are for shots with $B_0/n_e < 4 \times 10^{-14} \text{ kG cm}^3$.

The gross energy confinement time¹ $\tau_E = (3/2) \langle \beta \rangle_{vol} \tau_B^2$ can be calculated for each standard shot. Some discharges have bumps in the magnetic field decay¹ which prevents any measurement of τ_B^2 . The τ_E for the over 80 remaining shots is

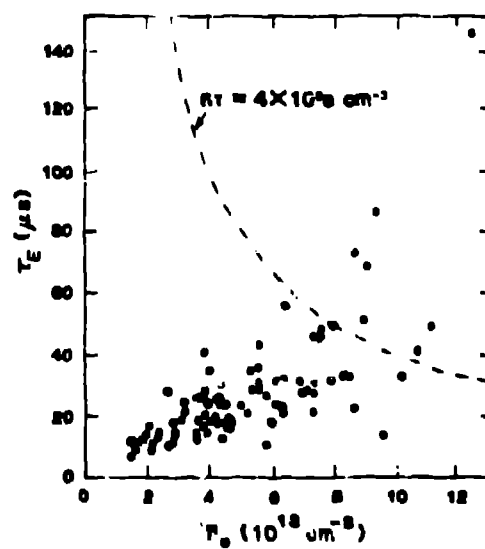


Fig. 5. Gross energy confinement time τ_E versus the line-averaged electron density at the time of the Thomson scattering data.

plotted versus the density in Figure 5. There appears to be a reasonably good correlation, with $\tau_E \propto n_e$. The value of $n\tau_E$ has reached $4 \times 10^9 \text{ s cm}^{-3}$. A temperature dependence is examined by dividing the τ_E by the density (to remove the assumed density dependence) and plotting the ratio versus the core T_e (Fig. 6). The confinement time appears to increase approximately linearly with T_e .

A zero-dimensional energy balance code, which accurately includes all the major atomic physics processes,¹⁰ is used to identify the causes of energy loss that contribute to the observed confinement time. The model includes equations for: electron, impurity, and neutral particle balance; magnetic field decay and ohmic power input; charge state evolution and radiation power loss; and electron and ion temperature balance. The parameters of the model are constrained by comparison to actual experimental data. An example is shown in Figure 7, where the standard mesh flux conserving discharges are modeled. The peak electron temperature is over 100 eV when the volume-average exceeds 40-50 eV. Constant particle confinement time

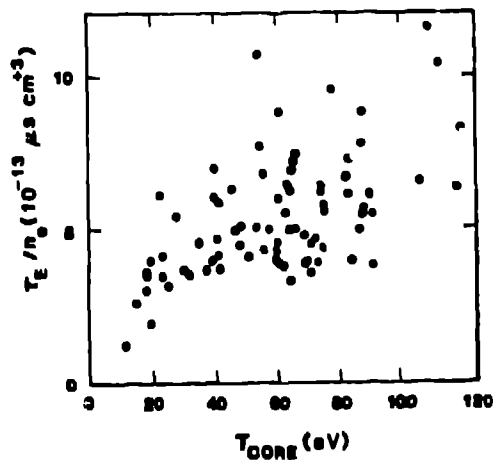


Fig. 6. τ_E divided by n_e versus the core temperature.

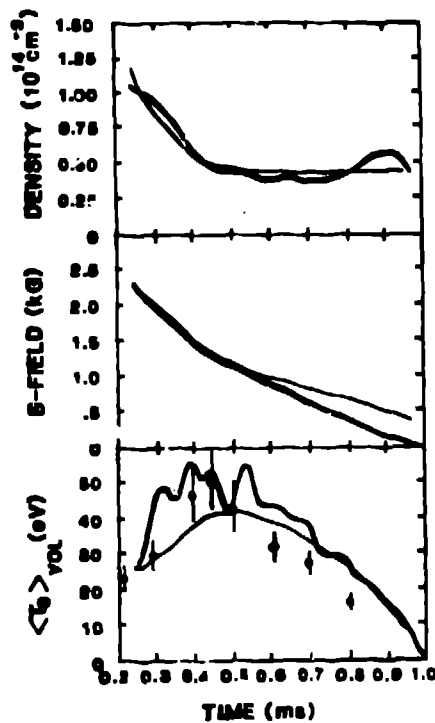


Fig. 7. Example of zero-dimensional modeling of mesh-flux-conserving decaying spheromaks. The bold lines are experimental data averaged from 15 shots in a typical day's run, while the light lines are the code results. The B-field is the volume-average, and the temperature is the conductivity value with $\kappa Z \ln \lambda = 65$. The temperature points are volume-average of Thomson scattering data, with 3-10 shots averaged at each time.

and neutral source rate have been assumed in the model, which only poorly models the cold, low-field termination of the discharge. Figure 8 illustrates the power balance of this example. At 0.6 ms the particle replacement power (the ionization and heating to the volume-average temperature of the neutrals needed to replace the particles being lost in order to maintain the constant density of the plateau) is becoming the dominant energy loss as the impurities "pump-out".³ The value of the ion temper-

ature, which is only ~ 15 eV in this example, is dependent upon the magnitude of the electron-ion coupling. This model can be used to estimate the behavior of future spheromak experiments which will depend critically on the value of the particle confinement time.

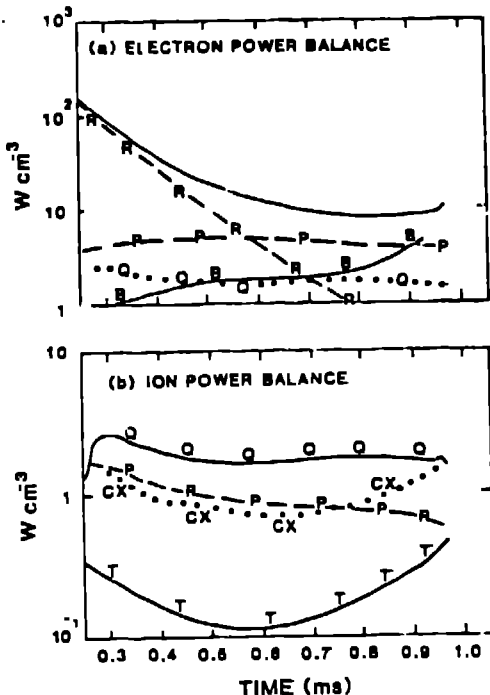


Fig. 8. Power densities versus time for the model of Fig. 7. (a) Solid line at top is ohmic power in. R-radiated power (9% oxygen/n_e initially). P-particle replacement power. B-Bohm-like thermal conduction loss. Q-classical e-i coupling. (b) CX-charge exchange power. T-classical ion conduction loss.

¹C. W. Barnes et al., "Spheromak Formation and Operation with Background Filling Gas and a Solid Lux Conserver in CTX," LA 1R-8-2422-Rev., accepted by Nuclear Fusion.

²R. Gribble et al., (to be published).

³T. R. Jarboe, C. W. Barnes, I. Henins, H. W. Hoida, S. O. Knox, R. K. Linford, and A. R. Sherwood, Physics of Fluids 27 (1984) 13.

⁴T. R. Jarboe, I. Henins, A. R. Sherwood, C. W. Barnes, and H. W. Hoida, Phys. Rev. Lett. 51 (1983) 39.

⁵H. W. Hoida et al., "Mixed Mode Operation in CTX", this conference.

⁶L. Spitzer, Jr., Physics of Fully Ionized Gases, (Interscience Publishers, New York, 1962).

⁷D. R. Wells and J. Norwood, Jr., J. Plasma Physics 3 (1969) 21.

⁸J. B. Taylor, Phys. Rev. Lett. 33 (1974) 1139.

⁹J. W. Finn, W. M. Manheimer, and E. Ott, Phys. Fluids 24 (1981) 1336. A. Bondaren et al., Phys. Fluids 24 (1981) 1682.

¹⁰C. W. Barnes et al., "Zero-Dimensional Time Dependent Energy Balance Modeling of CTX Spheromak Plasmas", 1983 IEEE International Conference on Plasma Science, San Diego, May 23-25, 1983, pg. 123 of Conference Record.